Superfluids

Eloi Estèvez Eki González Joan Pascual Timothy Skipper

January 29, 2025

Abstract

We make an introduction to the superfluidity phenomenon, focusing on the particular case of helium-II. Before this, we discuss the basics of Bose-Einstein condensation since this provides a better understanding of superfluidity as a quantum phenomenon. Additionally, we comment and justify the unique properties of He-II by performing our own simulation of the superfluid in which we observe some of these behaviors.

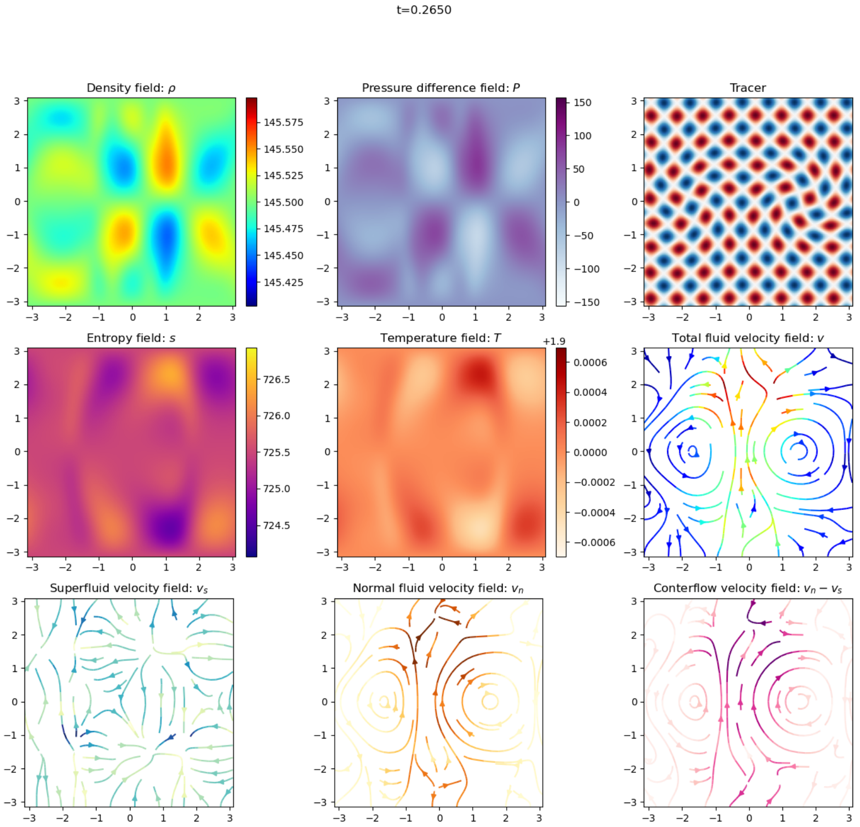

Contents

1 Bose-Einstein condensates

Before even talking about superfluids, we begin by investigating a quantum phenomenon called Bose-Einstein condensation. In essence, a Bose-Einstein condensate is a many-particle system which, due to certain conditions, can be described by a macroscopic wave function. The system exhibits properties different to classical solids, liquids and gases and thus is an entirely new state of matter.

In 1924 Satyendra Nath Bose was the first to study systems of particles with a symmetric wave function, now called bosons. He studied their statistical behavior and also considered the possibility of cooling down such a system to very low temperatures. He sent his work to Einstein for translation, who recognized the value of his efforts and agreed to translate the paper to German, also making his own contributions. Later, in 1938, Fritz London proposed that Bose and Einstein's ideas could apply to liquid helium and could be mechanism for its superfluidity.

1.1 Bose-Einstein statistics

Let us first consider a system of N bosons that do not interact with each other. Each individual particle can occupy one of several quantum states λ each with an energy ε_λ. λ may consist of one or multiple quantum numbers. Let n_λ be the number of particles in the state λ.

In Bose's paper, he determined an expression for the expected value of n_i, different to the Boltzmann distribution, because he used the fact that the particles are indistinguishable. For example, suppose we have two coins with two possible energy states, heads and tails. Classically, there are four possible scenarios, but for bosons, there are just three: HH, HT and TT (HT and TH are the same!) Thus some states are counted less than would be expected from a classical point of view. The Bose distribution is given by:

$$\langle n_\lambda \rangle = \frac{1}{e^{(\varepsilon_\lambda - \mu)/(k_B T)} - 1}$$

Here μ is the chemical potential and T the temperature of the system.

1.2 Ideal BEC

Now let us consider the system at low temperatures. We can write the wave function of the system as a product of individual wave functions:

$$\Psi(\mathbf{r}_1, \ldots, \mathbf{r}_N) = \varphi_{s_1}(\mathbf{r}_1) \cdots \varphi_{s_N}(\mathbf{r}_N)$$

This isn't entirely correct, however. Since the particles are bosons, the wave function Ψ must be symmetric. We can amend this by symmetrizing our function:

$$\Psi(\mathbf{r}_1, \ldots, \mathbf{r}_N) \propto \sum_\sigma \varphi_{s_1}(\mathbf{r}_{\sigma(1)}) \cdots \varphi_{s_N}(\mathbf{r}_{\sigma(N)})$$

Where σ is summed over the permutations of N objects. The proportionality factor can be determined if necessary.

For large N, the previous expression quickly becomes unwieldy and difficult to deal with. Fortunately there exists an alternative formalism of quantum mechanics, called **second quantization**, that greatly simplifies the treatment of many-particle systems. In 'first quantization', the system is expressed in terms of each particle j being in the state s_i: $\varphi_{s_i}(\mathbf{r}_j)$. In second quantization, however, we forget about the individuality of the particles and simply talk of *how many particles are in each possible state.* This is natural because the particles are indistinguishable anyway, and so we don't need to worry about symmetrizing (or antisymmetrizing for fermions) the wave function any more.

Let ψ_λ be the wave function for a single-particle system with the state λ. $\{\psi_\}$ is then a complete basis of wave functions. Now, the basis of states in second quantization are described by the set of non-negative integers $\{n_\lambda\}$, the occupation numbers. If we fix the total number of particles, N, we require $\sum_\lambda n_\lambda = N$.

What is the probability density of the state $\{n_\lambda\}$ at a point $\mathbf{r}$? For every state, there are n_λ particles in that state, and a probability density of $\psi^*_\lambda(\mathbf{r})\psi_\lambda(\mathbf{r})$ for every particle (assuming the ψ_λ's are normalized). So in total it will be $P(\mathbf{r}) = \sum_l n_l \psi^*_\lambda(\mathbf{r})\psi_\lambda(\mathbf{r})$.

Now our system is a Bose-Einstein condensate if it is at a low enough temperature that a large number of the particles are in the ground state, i.e. $n_0 \approx N$. This point is called the **critical temperature** of the condensate. In this case, $P(\mathbf{r})$ is determined mostly by the component $n_0\psi^*_0\psi_0$, and the others are small fluctuations which vanish as the temperature approaches 0. If we define $\Psi_0(\mathbf{r}) = \sqrt{n_0}\psi_0$, then the BEC is described in large part as if it were a single-particle system; thus, Ψ_0 is called the **macroscopic wave function**.

1.3 Interacting BEC

So far we have only been considering an ideal Bose gas with no interactions. In reality, the bosons do interact with each other. In 1956, Oliver Penrose and Lars Onsager proposed a criterion for when BEC occurs in general Bose gases. Essentially, it so happens that similar to the occupation numbers n_λ and the basis functions ψ_λ, one can define a certain series of numbers α_λ and functions ϕ_λ that are eigenvalues and eigenfunctions of a certain operator, and that they coincide with the n_λ's and the ψ_λ's for an ideal Bose gas. The Penrose-Onsager criterion, then, is that α_0 is close to N. In this case, the macroscopic wave function is $\sqrt{\alpha_0}\phi_0$.

1.4 Basic properties

The fraction of particles in the ground state, n_0/N can be determined statistically from the Bose-Einstein distribution. It only depends on the temperature, since this determines the average energy per particle. In 1995, when a BEC was created for the first time, this was experimentally confirmed (figure 1).

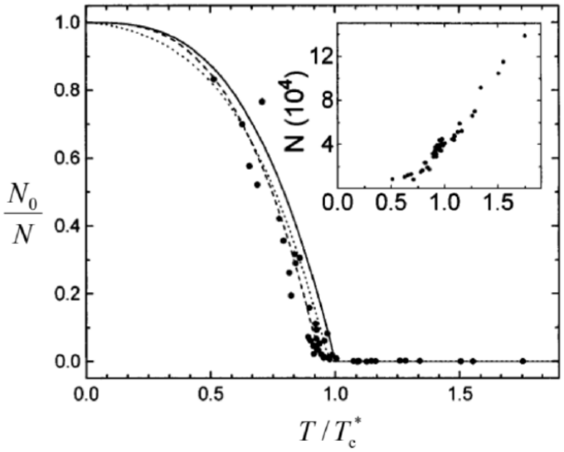

Figure 1: The condensate fraction of trapped rubidium atoms as a function of the temperature. The solid line shows the theoretical prediction, and the points represent the experimental data.
Source: [JREC96]

Thus we can think of this state of matter as having two components: the condensate, which consists of the particles in the ground state, and everything else, which create thermal fluctuations. Since the condensate is described by a single wave function, it has a coherent flow and no collisions, thus being frictionless. Additionally, since there is only one possible energy state for it to be in (all of the particles in the ground state), its entropy is zero. Thus all the entropy is carried by the excitation part. We will see how these properties are relevant when we come to superfluidity.

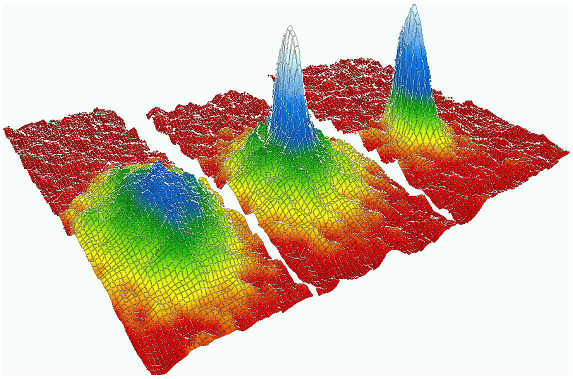

Figure 2: These graphs show the velocity distribution of the rubidium atoms at different temperatures in the same experiment. Left: 400 nK, just before the appearance of the BEC. Middle: 200 nK, just under the critical temperature. Right: 50 nK, the system is almost a pure condensate. This confirms the coherent flow due to the macroscopic wave function.
Source: [JREC96]

Nikolay Bogolyubov showed that for temperatures not too close to T_C one can make the approximation that the excitations behave like an ideal gas of quasiparticles, which are quantised Bogolyubov excitations. For details, see [BSP22] (1.1.4).

1.5 Vorticity

Another very striking property of BECs and also of superfluids is **quantum vorticity**. Take a superfluid at rest, and start rotating it, slowly accelerating. At first the liquid will simply stay at rest and not move at all. When a certain critical velocity is exceeded, however, small tornadoes will be visible in the fluid: these are the quantum vortices.

Later we will see that the superfluid is irrotational. Isn't this a contradiction with quantum vortices? No, because when a vortex occurs, a 'hole' appears in the macroscopic wave function, and the circulation of the velocity, $\kappa = \oint_C \mathbf{v}$ around the hole is non-zero (Stokes' theorem cannot be applied). The word quantum here means that κ is discrete, and in particular a multiple of h/m.

As a side note, this year quantum vortices have been experimentally observed for the first time in a supersolid, specifically made of dysprosium. (A supersolid presents many of the properties of superfluids, e.g. frictionless motion and quantum vortices, but retaining a more fixed atomic structure.)

1.6 Dynamics

Physicists Eugene Gross and Lev Pitaevskii deduced an equation that governs the macroscopic wave function of a pure condensate, that is, at $T = 0$. In this idealized system, the interaction between atoms is a contact potential (i.e. proportional to $\delta(\mathbf{r} - \mathbf{r}')$ with δ the Dirac delta). It is called the **Gross-Pitaevskii equation** or the non-linear Schrödinger equation:

$$-\frac{\hbar}{2m}\nabla^2\Psi + V\Psi + \frac{4\pi\hbar^2 a}{m}|\Psi|^2\Psi = i\hbar\frac{\partial\Psi}{\partial t}$$

Where Ψ is the macroscopic wave function, V is an external potential and a is a parameter that represents the strength of the contact potential.

An alternative way to model the dynamic behavior of the system is to find equations for its 'density' and 'velocity', similar to the way it is done in fluid dynamics, as we will see later. Recalling that $P(\mathbf{r}) = |\Psi_0(\mathbf{r})|^2$, it makes sense to call this the density of the condensate, n. It turns out that from the Gross-Pitaevskii equation one can deduce that:

$$\frac{\partial n}{\partial t} + \nabla \cdot (n\mathbf{v}) = 0$$

where $\mathbf{v}$ is some function equal to:

$$\mathbf{v} = \frac{\hbar}{2mi}\frac{\Psi * \nabla\Psi - \Psi\nabla\Psi *}{|\Psi|^2}$$

Now, as we will see in 3.1, the equation above is very similar to the continuity equation of a fluid. Thus, it makes sense to identify the field $\mathbf{v}$ with the velocity of the fluid. It can be verified that $\nabla \times \mathbf{v} = 0$, that is, we are talking of an ideal (irrotational) fluid that has a potential flow. In fact, it can be deduced, that the potential flow is in particular caused by the chemical potential:

$$\frac{\mathrm{D}\mathbf{v}}{\mathrm{D}t} = \frac{\partial \mathbf{v}}{\partial t} + (\mathbf{v} \cdot \nabla)\mathbf{v} = -\frac{1}{m}\nabla\mu \tag{1}$$

The derivations in this section are made, for instance, in [Tem] (1.4-1.5).

2 The discovery of superfluidity and its properties

2.1 Helium-II, an introduction

One of the most important properties of helium is that it cannot freeze at ambient pressure (25 atmospheres are required). It remains liquid for near-zero temperatures, contradicting the classical theory of matter. The explanation for this unique behavior lies in the Heisenberg uncertainty principle whose effects alter the energy of the system. This quantum principle gains importance for atoms with low mass and low potential, which is especially the case for the lightest of the noble gases. In such a way, at these scales, there is a kind of kinetic equilibrium for the so-called zero-point motion characterized by the minimum average total (potential + kinetic) energy.

As we shall see, the existence of superfluids such as liquid helium and, in particular, the strange mass and heat transfer mechanism they exhibit directly indicate that they represent a macroscopic system with some quantum properties because at these temperatures the mean thermal (kinetic) energy becomes so small that the mean de-Broglie wavelength $\lambda = h/p$ assumes a value of the order of the minimum molecular distance. So, the classical theory is incompetent and that presumably quantum mechanisms are relevant to their constitution as a whole.

Pioneers in cryogenics were interested in the problem of minimizing the temperature of helium. The first to liquefy helium at 4.2 K was Heike Kamerlingh in 1908. A couple of years later, he realized that below 2.17 K the violent boiling process disappeared radically, although there is still a phase change to vapor. In the same line, he found that it starts to expand instead of continuing to contract when temperature drops below this set value, thus deviating from the behavior of other substances.

The disappearance of the bubbles implies that there is no longer an irregular temperature distribution in the liquid. Now, if we place an electrical resistor in the helium below 2.17 K, it will dissipate the heat efficiently enough so that no bubbles appear.

This new state of helium became known as “Helium-II”. Willem Hendrik discovered that Helium-II was the best thermal conductor of all known materials, capable of flattening any thermal gradient. It has been shown that thermal conductivity of He-II is approximately 200 times higher than copper’s conductivity.

On the other hand, Kamerlingh Onnes and Leo Dana found that cooling was more difficult near the transition because of the sudden increase in specific heat. This phenomenon led to Keesom and Wolk in 1928 to define the terminology “helium I” and “helium II”, for the heater and cooler states respectively, suggesting the idea of a kind of allotropic modification. The silhouette of the specific heat peak gave the phase change between He-II and He-I its name: the lambda transition, which is the sharpest phase transition known to us. This result can be related to conclusions from the study of the specific heat of Bose gases near Bose-Einstein condensate temperatures.

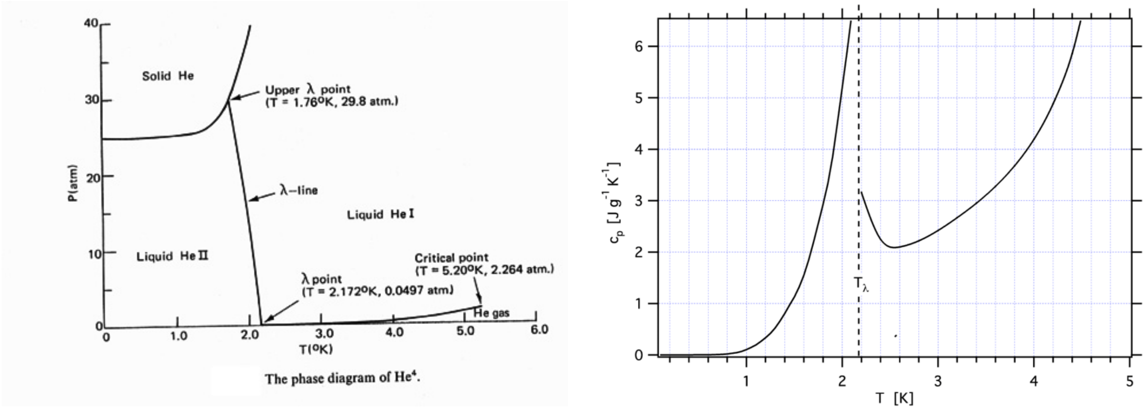

(a) Allocation of the four states of helium in the P-T plane

Source

(b) Specific heat of liquid helium under its own vapor pressure.

Source

Figure 3

2.2 Superflow

In 1930 Keesom and Van der Ende observed quite accidentally that liquid He-II passed with very annoying ease through extremely small leaks which at a higher temperature were perfectly tight for liquid He-I and even for gaseous helium.

But it was not until 1938 that the most important property of He-II was studied quantitatively. Researchers Jack Allen and Donald Misener, on the one hand, and Pjotr Kapitza, on the other, conducted experiments on the flow of He-II to conclude that it can flow without viscosity. It turns out that at temperatures below the lambda temperature, this substance presents (with current experiments) no difficulty in passing through capillaries of the order of nanometers. This phenomenon was named superfluidity. The ideal fluid behavior adds to the arguments in favor of He-II having a Bose condensate of He atoms.

We could conclude that this phenomenon is due to the disappearance of viscosity. However, nature is not so simple. Experimentally, using a viscometer, a gradual (not sudden) drop in viscosity is observed starting at T_λ.

The effects of this phenomenon will be discussed in more detail in future chapters.

2.3 Thermal Superconductivity

In 1936 Keesom and Miss Keesom noticed an enormous increase of heat exchange as liquid helium passes through the λ-point. In 1937 Allen, Peierls and Uddin first noticed that the heat current is liquid He-II is not proportional to the temperature gradient (violating the Fourier Law). In particular, it was shown to depend on the temperature of the liquid. More experimental evidence, such as the fact that at any rate the heat current depended on the slit width through which the liquid passed in a way that rules out a description by a heat conductivity equation.

Heat must be transported in another previously unknown way, a new mechanism. Thermal superconductivity is uniquely linked to superfluids, being as characteristic as superfluidity itself.

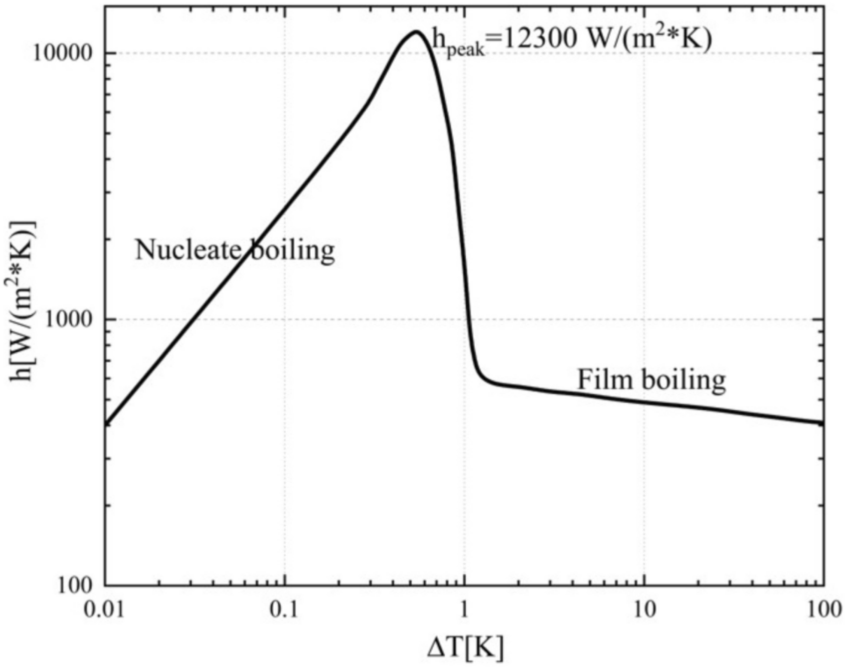

Figure 4: Heat transfer coefficient from a metal surface to liquid helium

Source

2.4 Entropy

By examining the phase diagram on P-T plane 3a, we can observe more conspicuous properties. Probably the most striking one might be the absence of a triple point between the solid, liquid and gaseous states. Instead are actually two triple points, at the ends of the λ-line which separates liquid He I from He II.

In addition, another peculiarity is that melting curve seem to approach $T = 0$ at a pressure of about 25 atm flattening in a asymptotic way. From the Clausius-Clapeyron equation $dP_m/dT = (S_{liq} - S_{sol})/(V_{liq} - V_{sol})$ where P_m is the melting pressure curve, it follows that at 1 K the entropy of the liquid must be practically equal to entropy of the solid, as $dP_m/dT = 0 \implies \Delta S = 0 \implies S_{liq} = S_{sol}$.

Hence, it seems as if between 2.2 K and 1 K liquid helium loses all entropy characteristic of the disorder of the ordinary liquid state.

Solid helium cannot be melted isothermally by supplying heat to the system, since there is no heat of melting. Close to absolute zero, solidification and melting are purely mechanical processes as no entropy change is involved in this transition.

2.5 Viscosity paradox

In 1938 Keesom and Macwood measured the viscosity with the rotation disk method and showed that the viscosity varies continuously, decreases with decreasing temperature quite considerably, and is certainly not very different from the viscosity of He-I. In 1938 Kapitza (and independently Allen and Misener 1938) reported measurements based on the capillary flow method which showed the viscosity of liquid helium dropping by many orders of magnitude to an immeasurably small value. These experiments certainly did not indicate the presence of a viscous, laminar or turbulent flow. They cannot be discussed on the basis of the ordinary differential equation of hydrodynamics.

At absolute zero, where the system is in its lowest (single) quantum state, melting must then consist in an adiabatic transformation of this quantum state. Even at finite temperatures, at which liquid He-II has some entropy, there is a very peculiar transfer process by which at least a part of the liquid can slip through the finest cracks and extremely narrow slits and capillaries, which for normal liquids are, in effect, impassable (figure 5a). This apparent zero viscosity is referred to as superfluidity.

We could try to interpret this nested behavior as a solid with such a high molecular volume that actually can flow.

However, in other experiments, such as measuring the torque of a rotating disk submerged in a tank of liquid helium, the existence of a non-zero viscosity was proved, contradicting the results of the capillary flow (figure 5b).

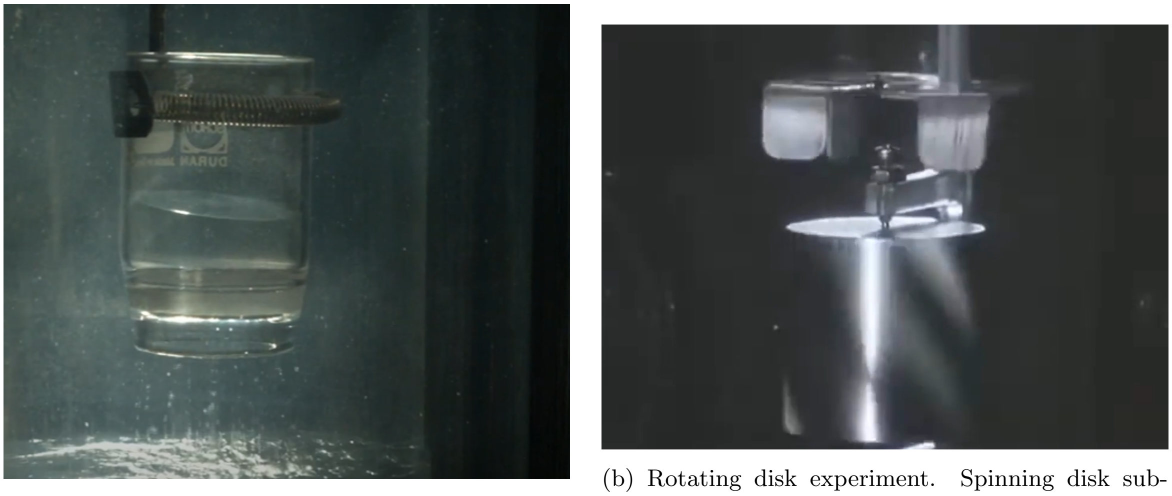

(a) Superfluid Helium drips as it flows through the capillaries

Source: El Hormiguero

(b) Rotating disk experiment. Spinning disk submerged in liquid Helium is able to transfer angular momentum to the top wheel.

Source: Alfred Leitner Liquid Helium II the Superfluid

Figure 5: Inviscid versus viscous behaviour of He-II

With this contradiction arises the first paradox. This substance, depending on the experiment performed, shows ideal (inviscid) or real (viscous) fluid behavior. But, as might be expected, the reality is more convoluted. Let's dig a little deeper.

This system does not represent a liquid in the ordinary sense. Unlike an ordinary liquid, there are no potential barriers to overcome when an external stress is applied. In this respect, there seems to be a greater similarity to a gas than we are used to assume in ordinary liquids. This view is supported by the extremely significant fact that liquid He-I, which at first sight appears to be quite an ordinary viscous liquid, actually has a viscosity of a type ordinarily found only in gases and not in liquids.

In ordinary liquids, the momentum transport proceeds over obstacles presumably formed by the interlocking force field of neighboring molecules. This can be derived from the fact that the viscosity of normal liquids has a large negative temperature coefficient, indicating that the passage of molecules between their neighbors is greatly aided by thermal excitation. $\eta_{liquid} \sim e^{A/RT}$ where A is the activation energy.

This liquid-type or dynamic viscosity is characteristically different from the gas-type or kinetic viscosity. In a gas, the transport of momentum proceeds without obstruction over the mean free path. It is proportional to the average momentum of the molecules and thus proportional to the square root of the temperature. $\eta_{gas} \sim \rho\overline{\nu}l \sim \sqrt{T}$ where $\overline{\nu}$ = average molecular velocity, l = mean free path, ρ = density. According to this formula, the viscosity of a gas increases with temperature.

As shown in figure 6a, the temperature coefficient of liquid He I is clearly positive and, hence, of the type usually shown only by gases. The viscosity of the liquid is only about 3 times that of that vapor, although its density is greater by a factor of 800: $\eta_{\text{He gas}} = 0.8 \times 10^{-5}$ poise and $\eta_{\text{He I}} = 2.5 \times 10^{-5}$ poise.

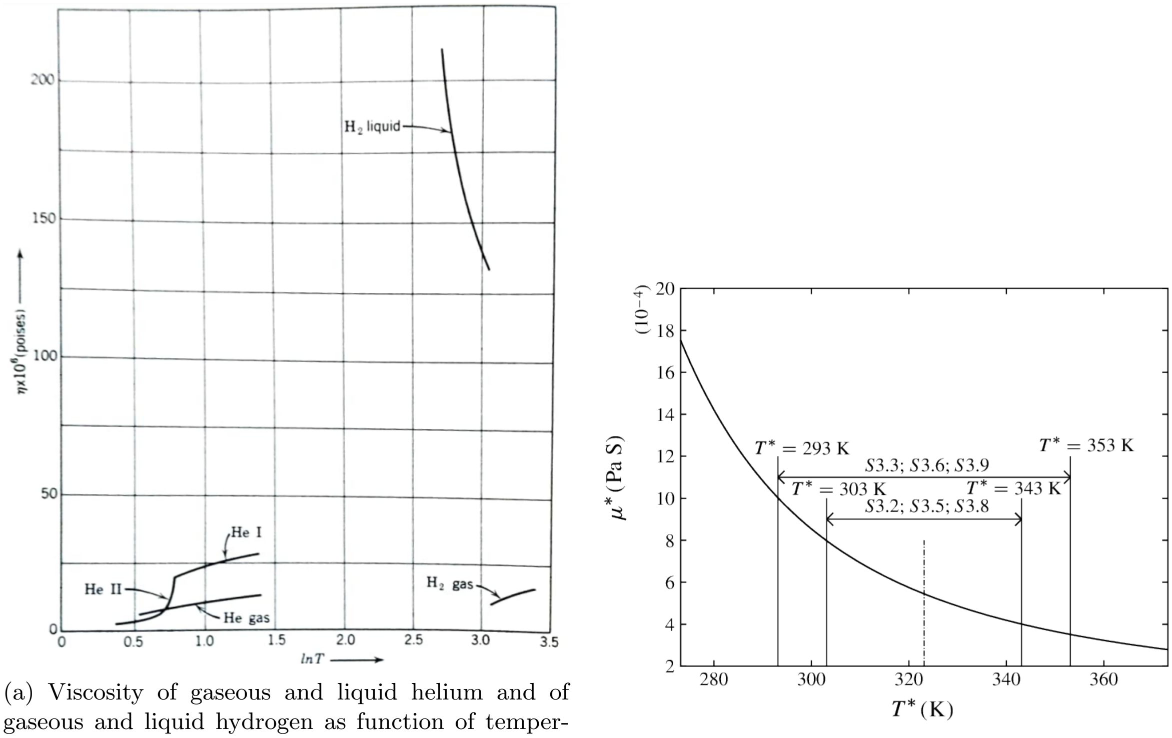

(a) Viscosity of gaseous and liquid helium and of gaseous and liquid hydrogen as function of temperature.

(b) Viscosity of water as a function of temperature.

Figure 6
Source: [Lon60]

Because of this exceptional large molar volume, liquid helium under low pressure might reasonably be contemplated from a point of view that emphasizes, more than usual with other liquids, the similarity to a gas. Only under sufficiently high pressure does liquid He-I behave like an ordinary liquid.

It appears that some aspects of liquid helium can be qualitatively explained by some classical models, but by putting the pieces together, nothing more than a paradoxical, counterintuitive chimera is obtained.

2.6 Notes on the Lambda transition

Ehrenfest, considering especially the λ-transition of liquid helium and the specific heat discontinuity of superconductors, introduced a general classification of "phase transitions of higher order". He speaks of a transition of the nth order if the Gibbs potential $G(P, T)$ has, at the transition line $P(T)$, a discontinuity of its nth partial derivatives, but not of a lower order derivative.

The **first order transitions** are the ordinary phase transitions with a transition heat accompanied by a change of molar volume, both quantities being connected with the slope of the transitions curve $P(T)$ by the Clausius-Clapeyron equation $dP/dT = \Delta S/\Delta V$ where ΔS and ΔV refer to the entropy and volume difference at the transitions in question. This relation follows directly from the continuity of the Gibbs potential at the transition line.

For the **second order transitions**, not only ΔG but also ΔS and ΔV are zero along the transition line. This has the consequence that $dP/dT = \Delta C_P/(TV) = \Delta\alpha_P/\Delta\chi_T$ where C_P is the specified heat at constant pressure, α_P is the thermal expansion coefficient at constant pressure, and χ_T is the isothermal compressibility. Hence here only C_P, α_P and χ_P are discontinuous.

Similar relations can be derived for higher order transitions. Although this classification appears to be quite general, it is difficult to apply to the λ-transition of liquid helium, although it was with just this transition in mind that the whole classification was devised.

As we had anticipated, in contrast to ordinary phase transitions, the transition from He-II to He-I was shown to not be accompanied by a latent heat. Later on, in 1932, specific heat measurements by Keesom and Clausius showed a singularity of the specific heat curve with the characteristic letter lambda shape profile.

The lambda-point occurs in many substances. It consists in transitions of second order which are characterized by vanishing latent heat and the above-mentioned sort of singularity of specific heat. They usually occur whenever some type of order is gradually destroyed with rising temperature, until, at some well-defined "transition temperature" the last vestige of this order disappears. A very well-studied example of this anomaly is the ferromagnetic Curie point of the metals of the iron group (figure 7a).

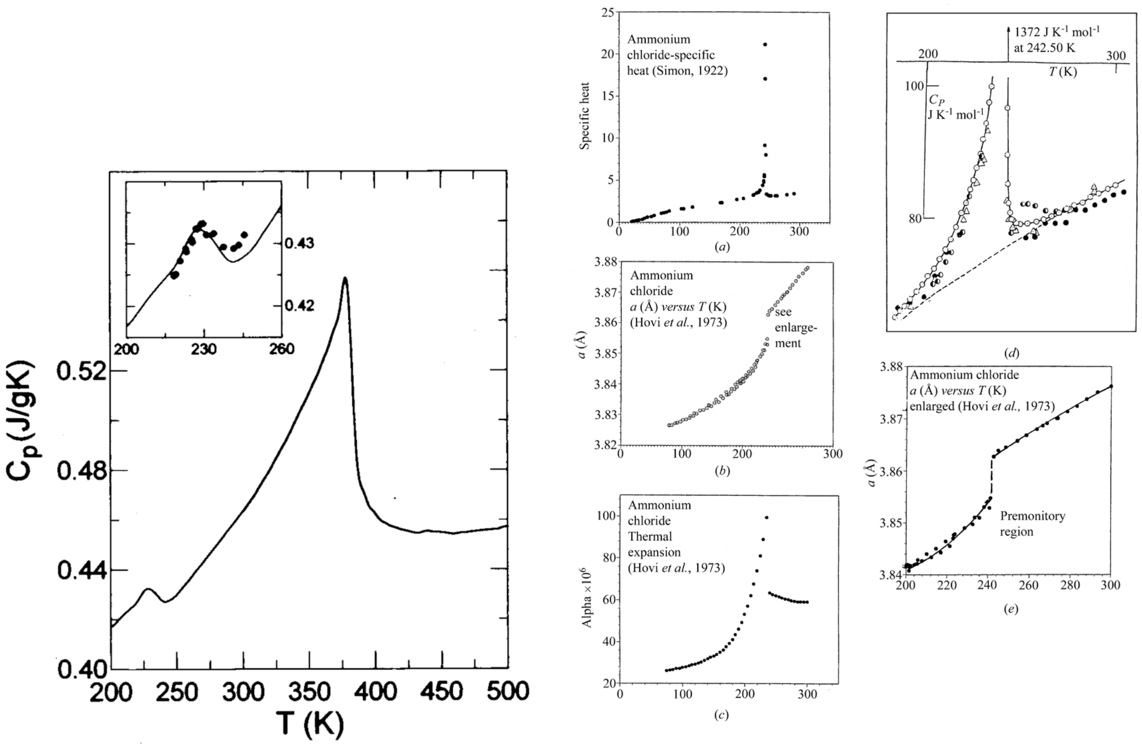

(a) Specific heat as a function of temperature showing the peak at the Curie point.
Source

(b) Several experiments on NH_4Cl showing discontinuity on the slope of various thermodynamic magnitudes.
Source

Figure 7

However, the classical example of the λ-point of liquid helium does not seem to admit an explanation in terms of any mechanism of this kind; the helium atoms are just too symmetrical to achieve an order-disorder transition, say, by virtue of an orientation like that of the NH_4 tetrahedra of the ferromagnetic dipole alignment. Nor can a pure substance like helium establish anything like the type or order of binary alloys. Liquid helium seems to be too simple to have a λ-point!

In fact, Bose-Einstein condensates also experience a lambda transition at the critical temperature. The interpretation of why this is the case could be that this transition, instead of being caused by the order-disorder transition in position space as for other substances, for Bose-Einstein condensates the transition occurs in momentum space. For a Bose gas of helium 4 atoms, one calculates lambda transition temperature of $T_\lambda = 2.16K$ which is extremely close to the experimental lambda temperature $T_\lambda = 2.17K$ ([Kru15]).

3 The two-fluid model

As we have seen in previous sections, Helium-II presents an apparent contradiction in its behavior under lambda temperature. In particular, depending on the experiment, it acts in a viscous or ideal manner. This “duality” may remind the reader of the wave-particle duality present in quantum mechanics. In fact, this is the culprit.

Laszlo Tisza introduced for the first time in 1938 the "two fluid model" of superfluidity. Tisza published the basics of his model as a note in *Nature.* In 1941, Lev Landau reformulated this model in a more rigorous manner. The idea of a mixture of two fluids with independent velocities was consolidated with successive experimental research. Their prediction of the existence of heat waves, as a consequence of the model, was also confirmed. After this, it took several decades for the superfluidity of liquid helium to be fully understood.

The Landau-Tisza model that we derive in this section is formulated in terms of five quantities (superfluid density ρ_s, normal density ρ_n, superfluid velocity v_s, normal velocity v_n and entropy density s). We immediately deduce four evolution equations, namely, the continuity equation, balance of momentum, evolution of superfluid velocity, and entropy balance. Since we have more variables than equations, we set a dependence on the ratio ρ_n/ρ on temperature.

However, the distinction between these two densities is not completely real. It actually goes against the nature of superfluid helium-II, which is a single fluid with two motions, as expressed by Landau: "It must be particularly stressed that we have here no real division of the particles of the liquid into 'superfluid' and 'normal' ones."

It must be mentioned that the model has several limitations. For instance, it does not allow for non-zero superfluid vorticity, which will not be treated here.

3.1 Introduction to classical fluid dynamics

Before delving into the equations of the two-fluid model, let us first get a brief overview of the equations that govern classical fluids. The classical theory of fluid dynamics generally assumes that the fluid is continuous and indivisible. This is of course not true since it is composed of molecules, but at human scales, where we are talking about 10^{23} particles, it turns out to be an excellent approximation.

We take the fluid to be located in a region V of space. Its state is described by the vector field of velocities $\mathbf{v}$ and the density field ρ. We can then describe its motion through a series of partial differential equations. Because we are assuming the fluid is continuous, we can suppose that $\mathbf{v}$ and ρ are smooth enough for the equations.

Firstly, we have the continuity of mass:

$$\frac{\partial \rho}{\partial t} + \nabla \cdot (\rho \mathbf{v}) = 0$$

The first term indicates the rate of change of mass at a point, and the second term represents the flux of mass leaving that point.

Secondly, we can use Newton's second law to derive a law of **balance of momentum**. This can be written as:

$$\rho \frac{\mathrm{D}\mathbf{v}}{\mathrm{D}t} = \mathbf{f}$$

where $\mathbf{f}$ is the total force per unit volume. Here we must use the total derivative $\mathrm{D}/\mathrm{D}t = \frac{\partial}{\partial t} + (\nabla \cdot \mathbf{v})$ since we are referencing the rate of change of the piece of fluid that is flowing with velocity $\mathbf{v}$.

- Conservative forces can be written as the gradient of a potential: $-\nabla \phi$.

- In an ideal fluid, the only forces are due to the pressure, $-\nabla p$ and the external body forces, $\rho\mathbf{b}$ where $\mathbf{b}$ is the body force per unit mass.
- In a real fluid there are additional forces due to viscosity. In the Navier-Stokes equation the viscous term is proportional to the Laplacian of the velocity:

$$\rho\frac{\mathrm{D}\mathbf{v}}{\mathrm{D}t} = -\nabla p + \rho\mathbf{b} + \eta\nabla^2\mathbf{v}$$

For more details, see [AJC93].

3.2 Two densities

Experimentally, physicists noticed that the existence of two components does not mean distinguishable fluids, since the superfluid behavior is not eliminated when He-II is filtered through the capillary! Therefore, these components can transform into each other, as if each particle had both natures.

This duality was studied by Elepter Andronikashvili in 1946. He constructed a stack of finely separated disks, which he attached to the ceiling of the experimental cell forming a torsional oscillator. The frequency of oscillation is $\omega = \sqrt{\kappa/I}$, where κ is the stiffness coefficient of the string and I is the moment of inertia of string and disks. By measuring the frequency we can find the moment of inertia, he noticed that while the viscous fluid contributes to the moment of inertia, the superfluid component does not. Andronikashvili was thus able to measure the fraction that remained viscous, establishing the dependence of this ratio on temperature.

It is then concluded that the total density can be understood as the sum of superfluid component (non-viscous and does not allow temperature gradients) and a normal (viscous) component.

$$\rho = \rho_s + \rho_n$$

The superfluid part appears at lambda temperature and increases its presence with decreasing temperature until at near zero temperature the normal part is negligible. The normal component has non-zero thermal resistance, but this acts in parallel with the other, resulting in the discontinuity of thermal gradients observed in T_λ.

It should be emphasized that the fraction of each component is a function of temperature only (at a fixed pressure). If you had more normal component concentration in one part of the fluid then this would imply a thermal gradient which we have concluded is impossible.

3.3 Superfluid, microscopically

Let's understand why the two-fluid model is justified under quantum physics. Recall our discussion on Bose-Einstein condensates. The superfluid is a many-particle system which similar to a BEC is at a low temperature. Each individual particle may oscillate between different states, but at any one moment, most of them are in the ground state.

In a similar way that a macroscopic description of fluid dynamics treats the fluids like continuous substances with a velocity and density defined at each point, it is natural to describe the superfluid macroscopically by having two velocities and two densities associated with the macroscopic wave function, on the one hand, and the thermal fluctuations, on the other.

The reason that the two components are indistinguishable is that any one particle can oscillate between forming part of the superfluid and the normal fluid. It is the statistical fraction of particles in the ground state that provide the superfluid density, ρ_s. Since n_0/N only depends on the temperature, it makes sense that ρ_s/ρ would too.

3.4 Equations of superfluids

The main objective of this section is to find the correct equations for both components of Helium-II.

Given the two components of Helium-II, we can also separate the current density:

$$\mathbf{j} = \rho_s \mathbf{v_s} + \rho_n \mathbf{v_n}.$$

From the previous section we know that if we had momentarily a point with low superfluid density, this would be a hot spot, but quickly the thermal irregularity would be removed implying a net incoming flow of superfluid. In short, the superfluid flows from the cold side to the hot spot. Thermodynamically, this can only mean that this part carries zero entropy, so there can be no heat flow from cold to hot.

The lambda peak, zero entropy, frictionless flow, together with the increase of condensed (superfluid) particles with decreasing temperature, leads us to conclude that we have before us a Bose-Einstein condensate!

The normal component presents a nature that can be interpreted as the gas of Bogoliubov excitations on top of the condensate.

We recall the hydrodynamic equation for a condensate for the superfluid component. Also known as the Euler equation (1):

$$\frac{\partial \mathbf{v_s}}{\partial t} + (\mathbf{v_s} \cdot \nabla)\mathbf{v_s} = -\frac{1}{m}\nabla\mu$$

Where μ is the chemical potential, which we derive thermodynamically as follows. The chemical potential in terms of pressure and temperature is related with the Gibbs energy:

$$G(N, p, T) = N\mu(p, T)$$

Where N is the number of particles. In a differential form:

$$Nd\mu(p, Y) = \left.\frac{\partial G}{\partial p}\right|_T + \left.\frac{\partial G}{\partial T}\right|_p dT = Vdp - SdT$$

We have used the well-known definition of Gibbs energy and the relation:

$$G = VP - ST - TS = \mu N$$

Therefore, writing

$$\rho = (Nm)/V \qquad s = \frac{S}{mN}$$

We finally have

$$\nabla\mu = \frac{m}{\rho}\nabla\rho - ms\nabla T$$

Now, by direct substitution:

$$\frac{\partial \mathbf{v_s}}{\partial t} + (\mathbf{v_s} \cdot \nabla)\mathbf{v_s} = -\frac{1}{\rho}\nabla p + s\nabla T \tag{I}$$

However, the whole fluid has viscosity, so we need the Navier-Stokes equation:

$$\rho_s \left(\frac{\partial \mathbf{v}_s}{\partial t} + (\mathbf{v}_s \cdot \nabla)\mathbf{v}_s \right) + \rho_n \left(\frac{\partial \mathbf{v}_n}{\partial t} + (\mathbf{v}_n \cdot \nabla)\mathbf{v}_n \right) = -\nabla p + \eta_n \nabla^2 \mathbf{v}_n \tag{II}$$

where η_n is the viscosity of the normal component.

Subtracting the equation for the superfluid part (I) from the equation of the entire fluid (II) in order to isolate the hydrodynamic equation of the normal component:

$$\rho_n \left(\frac{\partial \mathbf{v}_n}{\partial t} + (\mathbf{v}_n \cdot \nabla)\mathbf{v}_n \right) = \left(\frac{\rho_s}{\rho} - 1 \right) \nabla p - \rho_s s \nabla T + \eta_n \nabla^2 \mathbf{v}_n$$

Here the four unknowns are ρ_s, ρ_n, $\mathbf{v}_s$, and $\mathbf{v}_n$. Therefore, we need two more equations. One of them is the continuity equation $\partial\rho/\partial t + \nabla \cdot \mathbf{j} = 0$, where we define $\mathbf{j} = \rho_s \mathbf{v}_s + \rho_n \mathbf{v}_n$. Note that we impose conservation for the total mass density instead of doing it for both components separately, because of the plausible transformation between them. In addition, we can impose the entropy transport continuity equation $\partial(\rho s)/\partial t = -\nabla \cdot (\rho \mathbf{v}_n)$.

Now we have closed the system of hydrodynamic equations for He-II, known as the two-fluid model:

$$\rho_s \left(\frac{\partial \mathbf{v}_s}{\partial t} + (\mathbf{v}_s \cdot \nabla)\mathbf{v}_s \right) = -\frac{\rho_s}{\rho}\nabla p + \rho_s s \nabla T, \tag{2}$$

$$\rho_n \left(\frac{\partial \mathbf{v}_n}{\partial t} + (\mathbf{v}_n \cdot \nabla)\mathbf{v}_n \right) = -\frac{\rho_n}{\rho}\nabla p - \rho_s s \nabla T + \eta_n \nabla^2 \mathbf{v}_n, \tag{3}$$

$$\frac{\partial(\rho_s + \rho_n)}{\partial t} = -\nabla \cdot \mathbf{j}, \tag{4}$$

$$\frac{\partial(\rho s)}{\partial t} = -\nabla \cdot (\rho \mathbf{v}_n). \tag{5}$$

This set of equations describe (with the appropriate boundary conditions) all special properties of He-II. In order to consider external potentials, we can simply add their potential energy per unit volume to the pressure term.

Finally, it must be remarked that this model is considered phenomenological. Landau and Tisza did not work out any microscopic interpretation.

4 Superfluid phenomena

In this section we will discuss the most impressive phenomena of superfluid helium. We will try to understand them by means of the already presented interpretation of the two-fluid model.

4.1 Fountain effect

One of the most fascinating phenomena presented by He-II is the fountain effect. A porous-based flask is immersed in a bath of He-II so that only the superfluid component can infiltrate the vessel. A heat source (such as a dissipative wire) is placed inside the flask. This heats the helium, causing the superfluid part to flow into the hot spot, causing the helium height to rise. This rise can reach the top of the bottle, escaping through a small hole made there, so that a fountain is observed. In short, a temperature gradient leads to a pressure head.

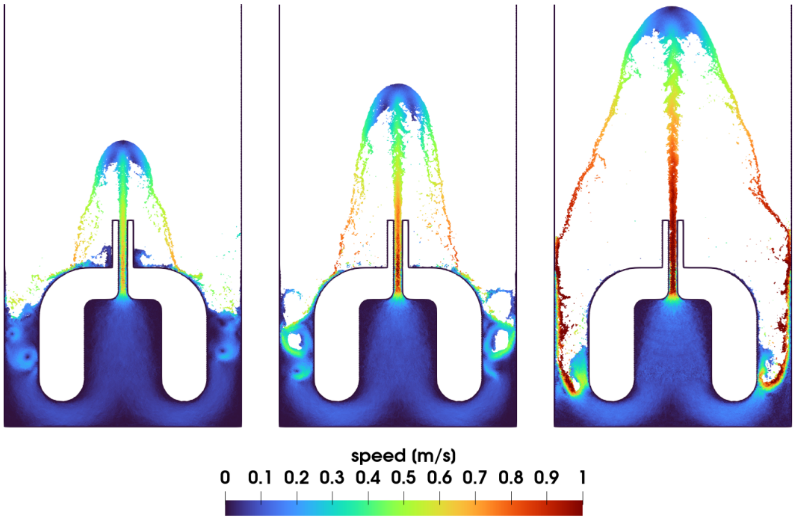

Figure 8: Simulation of Fountain effect using SPH at [KSP23]

Let's do some calculations. The pressure gradient can be extracted from equation (2) if we consider stationary regime, the partial with respect to time in LHS disappears. We assume now also that there is no fountain and we have a column (this tells us how tall a column would have to be for there to be no fountain effect), which allows us to simplify $\mathbf{v}_s = 0$ so that $\Delta p = \rho s \Delta T$, which is known as the fountain formula of Fritz London. Taking $\Delta p = mg\Delta h$, we see that for a $\Delta T \sim T_\lambda$ the corresponding height would be more than 50 meters, which is much higher than a common flask. In conclusion, a tiny temperature variation is enough to have a noticeable fountain.

This effect is simulated and studied in [KSP23], where they use the technique smooth particle hydrodynamics (figure 8).

4.2 Superfluid creep

This phenomenon appears when a cup is immersed in He-II and then removed from the liquid. Then, the helium inside the cup starts to rise on the inner surface of the cup, and goes down on the outside, so that it creates a layer covering the entire surface. Continuously, the fluid inside the cup travels through this coating to the bottom outside of the vessel, where droplets form and eventually drip out, emptying the vessel. In addition, the surfaces remain covered with a thin helium film after this process. The tendency of the fluid to cover the entire surface with which it comes into contact is called superfluid creep.

Superfluid creep is the consequence of the property of helium to maintain capillary flow through narrow channels. With a regular fluid (such as water), a meniscus is also observed due to the adhesion of the liquid with the vessel wall. However, as this layer is very narrow, there is an impediment to viscous flow. In addition, this film is very unstable in the face of temperature variations that evaporate and destabilize it. The capillary flow capability and superb thermal conductivity of He-II allow it to avoid these restrictions. Superfluid flow is possible, allowing the two phases to rise (remember that they are inseparable).

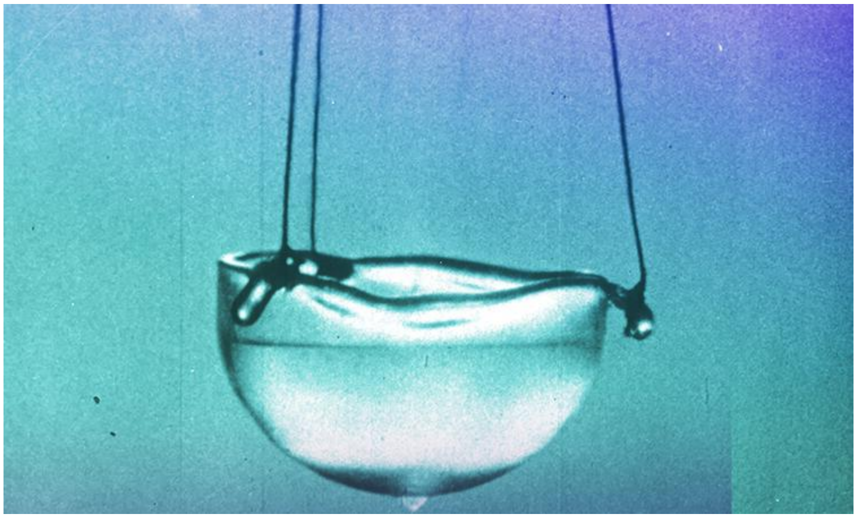

Figure 9: Capture of superfluid creep
Source: https://funsizephysics.com/superfluid-helium-black-holes/

4.3 Second sound

The phenomenon of second sound was first described by Lev Landau in 1941. [Lan41] So far, we have described several phenomena related to the unusual heat propagation in He-II, such as the absence of boiling, the fountain effect or superfluid creep. In normal fluids, the heat equation is one of diffusion giving rise to dissipative processes in which excess heat is transported over a distance that grows with the square root of time. However, in He-II, this heat propagates as a wave, so that the distance the heat is transported is linear with time. The temperature wave is called the second sound. Its velocity characterizes the speed with which the helium makes the temperature gradients disappear.

5 Our simulation

5.1 The model

Our simulation uses the model from [KSP23] which consists of the following four equations:

$$\frac{D\rho}{Dt} = -\rho \nabla \cdot \mathbf{v}, \tag{6}$$

$$\frac{Ds}{Dt} = -\frac{1}{\rho}\nabla \cdot (\rho s \chi_s \mathbf{v_{ns}}) + \frac{\beta}{\rho}\Delta T + \frac{\zeta}{\rho T}, \tag{7}$$

$$\frac{D\mathbf{v}}{Dt} = -\frac{1}{\rho}\nabla \cdot (\rho \chi_n \chi_s \mathbf{v_{ns}} \otimes \mathbf{v_{ns}} + p\mathbf{I}) + \frac{2\mu}{\rho}\nabla \cdot \mathbf{D_n} \tag{8}$$

$$\frac{D\mathbf{v_s}}{Dt} = \chi_n \nabla \mathbf{v_n}^T \mathbf{v_{ns}} - \frac{\nabla p}{\rho} + s\nabla T \tag{9}$$

Where the variables of our simulation $\rho, s, \mathbf{v}, \mathbf{v_s}$ are the density, specific entropy, coflow velocity, and superflow velocity, respectively. T, p, χ_n, χ_s are the temperature, pressure, and the mass fractions of normal and superfluid components. $\mu > 0$ and $\beta > 0$ are the dynamic viscosity and diffusion parameters respectively,

$$\mathbf{D_n} = 1/2(\nabla \mathbf{v_n} + \nabla \mathbf{v} - \mathbf{n}^T)$$

is a normal velocity deformation tensor, and

$$\zeta = \beta |\nabla T|^2 + 2\mu |\mathbf{D_n}|^2$$

is the dissipative power.

The coflow velocity $\mathbf{v}$ and counterflow velocity $\mathbf{v_{ns}}$ satisfy the following relations:

$$\mathbf{v} = \chi_n \mathbf{v_n} + \chi_s \mathbf{v_s}$$

$$\mathbf{v_{ns}} = \mathbf{v_n} - \mathbf{v_s}$$

The equations of the model contain convective derivatives with respect to the overall coflow velocity

$$\frac{D\phi}{Dt} := \frac{\partial \phi}{\partial t} + v \cdot \nabla \phi$$

This is the difference with respect to the Landau-Tisza model where the superfluid velocity is convected only by itself and not by the whole coflow velocity.

Closing the system of equations, requires the knowledge of functions p, T, and χ_n. Since the temperature gradient is small, we can use a linearized model, which is valid in a vicinity of a referential temperature T_0.

$$\chi_n = \chi_{n0} + \chi'(s - s_0), \tag{10}$$

$$\chi_s = \chi_{s0} - \chi'(s - s_0), \tag{11}$$

$$p = u_1^2(\rho - \rho_0), \tag{12}$$

$$T = (1 + \frac{s - s_0}{C})T_0, \tag{13}$$

Where $\chi', \chi_{n0}, \chi_{s0}, s_0, \rho_0, u_1$ and C are constant values at T_0 being u_1 the speed of sound and C the heat capacity.

The speed of the second sound u_2 is related to these values by:

$$u_2^2 = \frac{\chi_{s0} T_0 s_0^2}{\chi_{n0} C}$$

5.2 Method

In this section we briefly describe how we coded our simulation. A spectral method discretizes functions by expanding them over a set of basis functions.

Project Dedalus [BVO$^+$20] is a flexible framework for spectrally solving differential equations. We used this framework to spectrally solve the equations of our model over periodic 2D space.

We begin by defining the domain of our problem. Since we won't be imposing boundary conditions, our domain is defined with two-dimensional cartesian coordinates over the real Fourier basis. Next, we define the fields for the variables of our problem $\rho, s, \mathbf{v}, \mathbf{v_s}$ and the constants χ', χ_{n0}, χ_{s0}, s_0, ρ_0, u_1, C and T_0. Then, we define our initial value problem and the necessary substitutions to compute the operations of our model. We add the equations of the model and set the initial conditions. Finally, we build our solver, iterate for a certain simulation time and plot the results.

5.3 Simulations

In this section we show some results of the programming work we have done. In each simulation, we can see the manifestation of some property of helium-II discussed throughout this paper.

5.3.1 Simulation 1: First and second sound

In this first simulation we aim to observe the first and second sound and compare their velocities.

We found that if we set the initial velocity to $\mathbf{v} = (e^{-10x^2}, 0)$ a density and an entropy gradient is generated at he $x = 0$ line. In the density field, this gradient forms into a high density wave traveling to the right and a low density wave traveling to de left. We measured the speed of these waves to be around 40 m/s (since they take around 0.16 s to travel a distance of 2π) which matches the speed of sound. Similarly, in the entropy field we see a high entropy wave traveling to the right and a low entropy wave traveling to the left, the speed of these waves is around 19 m/s which matches the speed of the second sound which is 18.8 m/s.

5.3.2 Simulation 2: Peak in density

In the next two simulations, we will explore what happens when we add a perturbation to the density or entropy field.

In simulation 2 we set the initial density to $\rho = \rho_0 + e^{-10x^2}$ and observed how this perturbation in the density field creates a perturbation in the entropy field. In the density field, the peak in density divides in two high density waves, one traveling to the left and the other one traveling to the right.

In the entropy field, at the beginning we see an increase in entropy at the origin followed by a zone of low entropy which is then followed by another zone of high entropy. Then, as the simulation advances, we observe two waves in each direction, one of the form of a high to low perturbation and the other of the form of a low to high perturbation. One of these waves follows the density waves, traveling at the speed of sound and the other one stays behind, traveling at the speed of the second sound.

In figure 11 we can see some snapshots of the simulation.

5.3.3 Simulation 3: Peak in entropy

In simulation 3 we set the initial entropy to $s = s_0 + e^{-10x^2}$.

In figure 12 we can see a similar phenomenon to simulation 2, in this case, there are two waves in the density field, one follows the entropy traveling at the speed of the second sound and the other travels ahead of it at the speed of sound.

5.3.4 Simulation 4: Standing waves

In this simulation we set the velocity field to $\mathbf{v} = (0.1\cos(y), -0.1\cos(x))$ and found that both the density and the entropy fields oscillate in a certain pattern. If we measure the frequency of these oscillations, the density field has a frequency of around 8.8 Hz and the entropy field has a frequency of around 4 Hz. Since the oscillations are of the form $\cos(x + y) - \cos(x - y)$ we found reasonable that the wavelength would of $\sqrt{2}\pi$ m. With this assumption, we find that the velocity of the waves in the density field is 39 m/s and the velocity of the entropy waves is 17.7 m/s. This result agrees with the known speeds of the first sound (40 m/s) and the second sound (18.8 m/s).

Another property of superfluids that we can observe in this simulation is that the superfluid component is irrotational. In figure 13 we can see some snapshots of this simulation.

5.3.5 Simulation 5: Fountain effect

The objective of this simulation is to represent the fountain effect. As initial conditions, we set the entropy field to $s_o + 100e^{-(x^2+y^2)}$. With these conditions, we can clearly see the flow of the superfluid component towards the hot spot thus flattening the gradient of entropy and increasing the pressure and density. In figure 14 we have some images from this simulation.

6 Conclusion

In this project, we have seen a great variety of unusual and exciting behaviors of superfluid helium and how they can be modeled using a quantum theory of Bose-Einstein condensation. We also put the theories to the test by simulating such a fluid in a two-dimensional periodic environment, confirming some of these properties. We have been able to verify the phenomenon of second sound and confirmed that its velocity is roughly one half of that of first sound. In addition to this, we confirmed the thermomechanical effect and that the superfluid is irrotational. Some properties, such as superfluid creep and the dual viscous-inviscid nature of the fluid were outside of the scope of our simulation, since we had no boundary conditions in place and the simulation was only in two dimensions. Quantum vortices were also not present due to the macroscopic approximations made.

7 Acknowledgments

Special thanks to Ondrej Kincl, University of Trento. It has been a pleasure to correspond with a first class researcher. He has helped us to understand his paper and has been a motivation as a first contact with the more collaborative part of scientific research.

References

[AJC93] Jerrold E. Marsden Alexandre J. Chorin. *A Mathematical Introduction to Fluid Mechanics*. Springer, 1993.

[BSP22] Egor Babaev Boris Svistunov and Nikolay Prokof'ev. *Superfluid States of Matter*. CRC Press, November 2022.

[BVO$^+$20] Keaton J. Burns, Geoffrey M. Vasil, Jeffrey S. Oishi, Daniel Lecoanet, and Benjamin P. Brown. Dedalus: A flexible framework for numerical simulations with spectral methods. *Phys. Rev. Res.*, 2:023068, Apr 2020.

[JREC96] M. R. Matthews C. E. Wieman J. R. Ensher, D. S. Jin and E. A. Cornell. Bose-einstein condensation in a dilute gas: Measurement of energy and ground-state occupation. *Phys. Rev.*, 77:4984, 1996.

[Kru15] Vladimir I. Kruglov. Lambda transition and bose-einstein condensation in liquid $^4He. arxiv.org$, 2015.

[KSP23] Ondřej Kincl, David Schmoranzer, and Michal Pavelka. Simulation of superfluid fountain effect using smoothed particle hydrodynamics. *Physics of Fluids*, 35(4):047124, 04 2023.

[Lan41] L. Landau. Theory of the superfluidity of helium ii. *Phys. Rev.*, 60:356–358, Aug 1941.

[Lon60] Fritz London. *Superfluids: Macroscopic theory of superfluid helium.* New York, Dover, 1960.

[Tem] Jacques Tempere. Bose-einstein condensation, superfluidity and superconductivity. *Course notes.*

A Appendix: Simulation snapshots

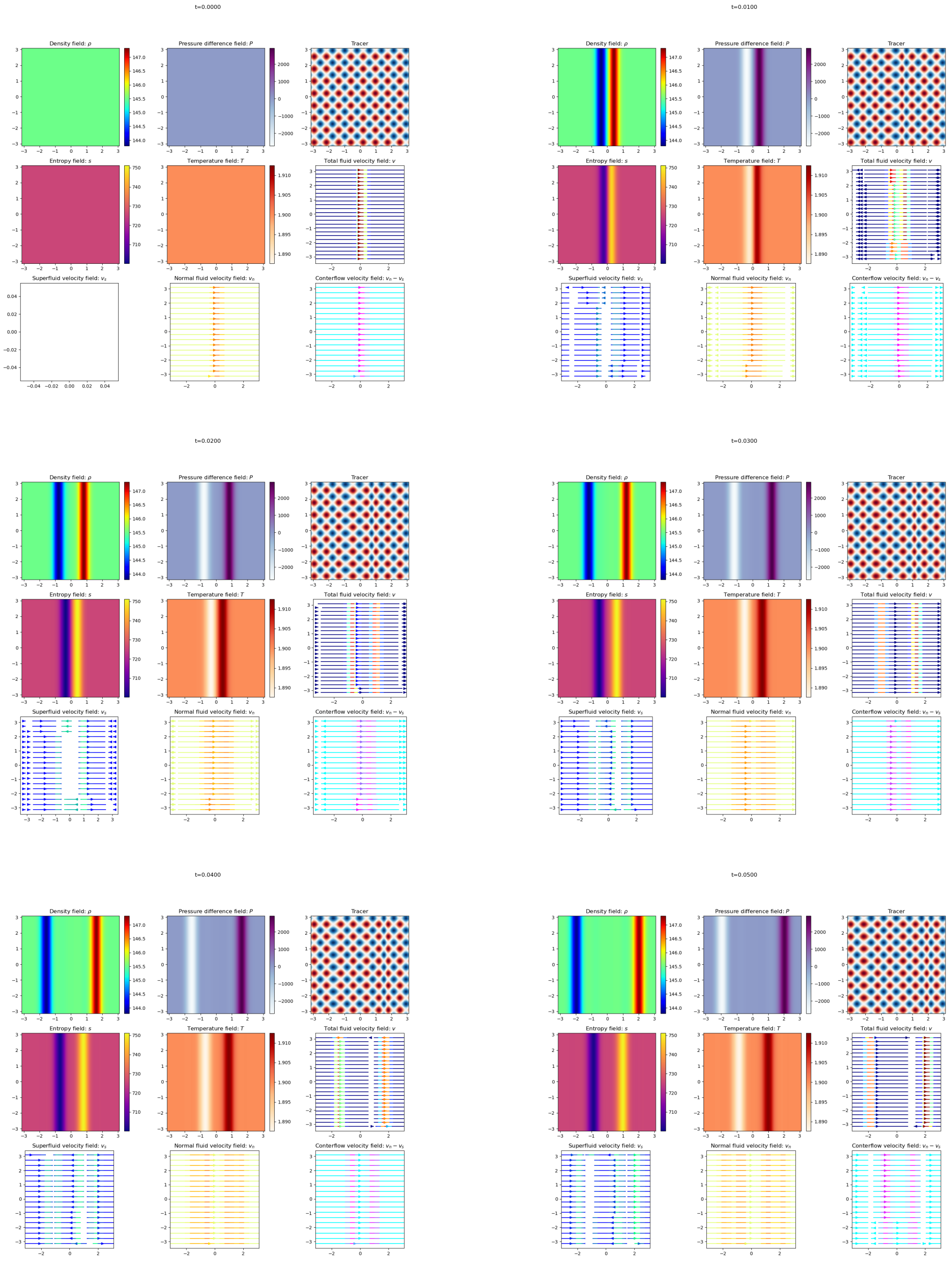

Figure 10: Snapshots from simulation 1

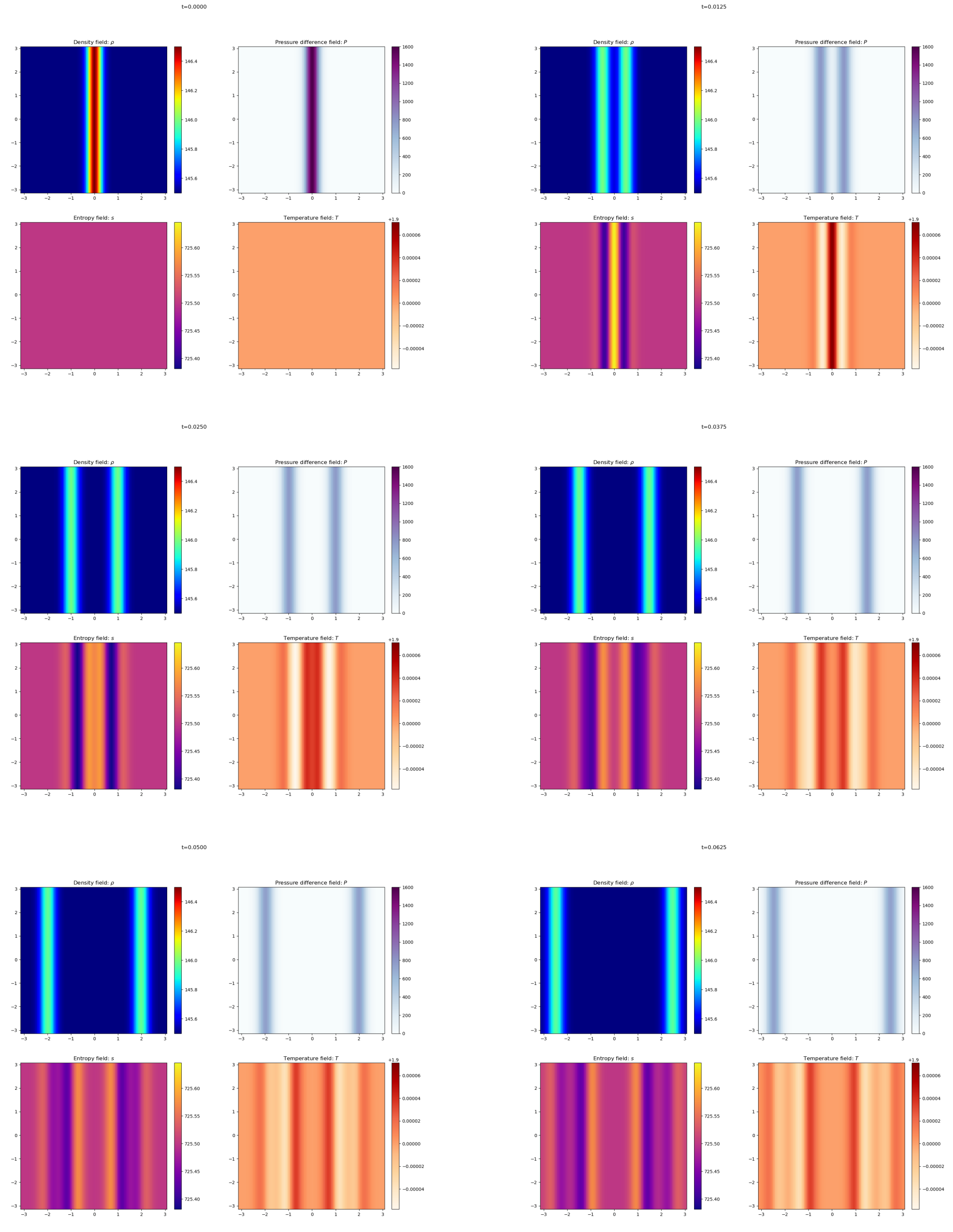

Figure 11: Snapshots from simulation 2

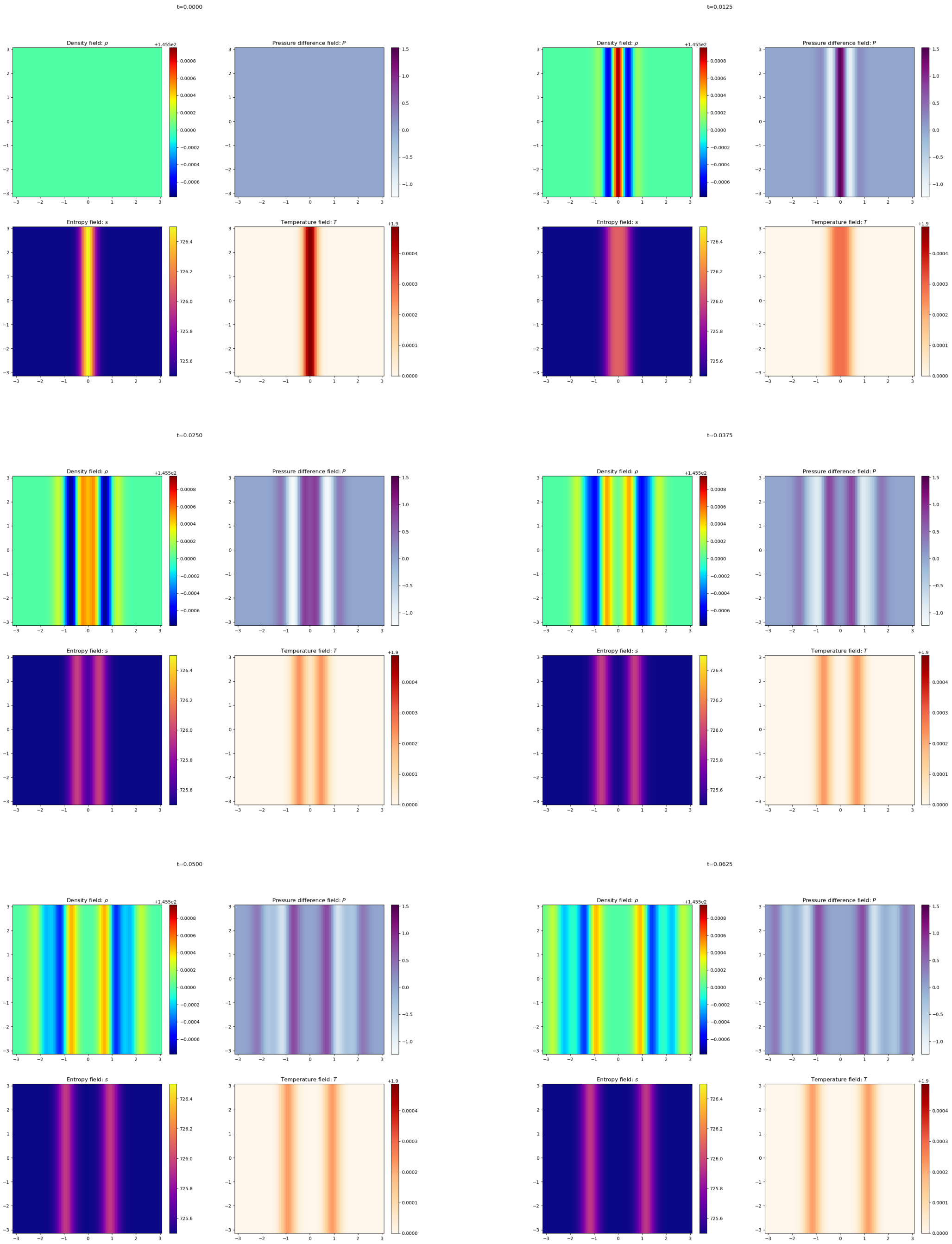

Figure 12: Snapshots from simulation 3

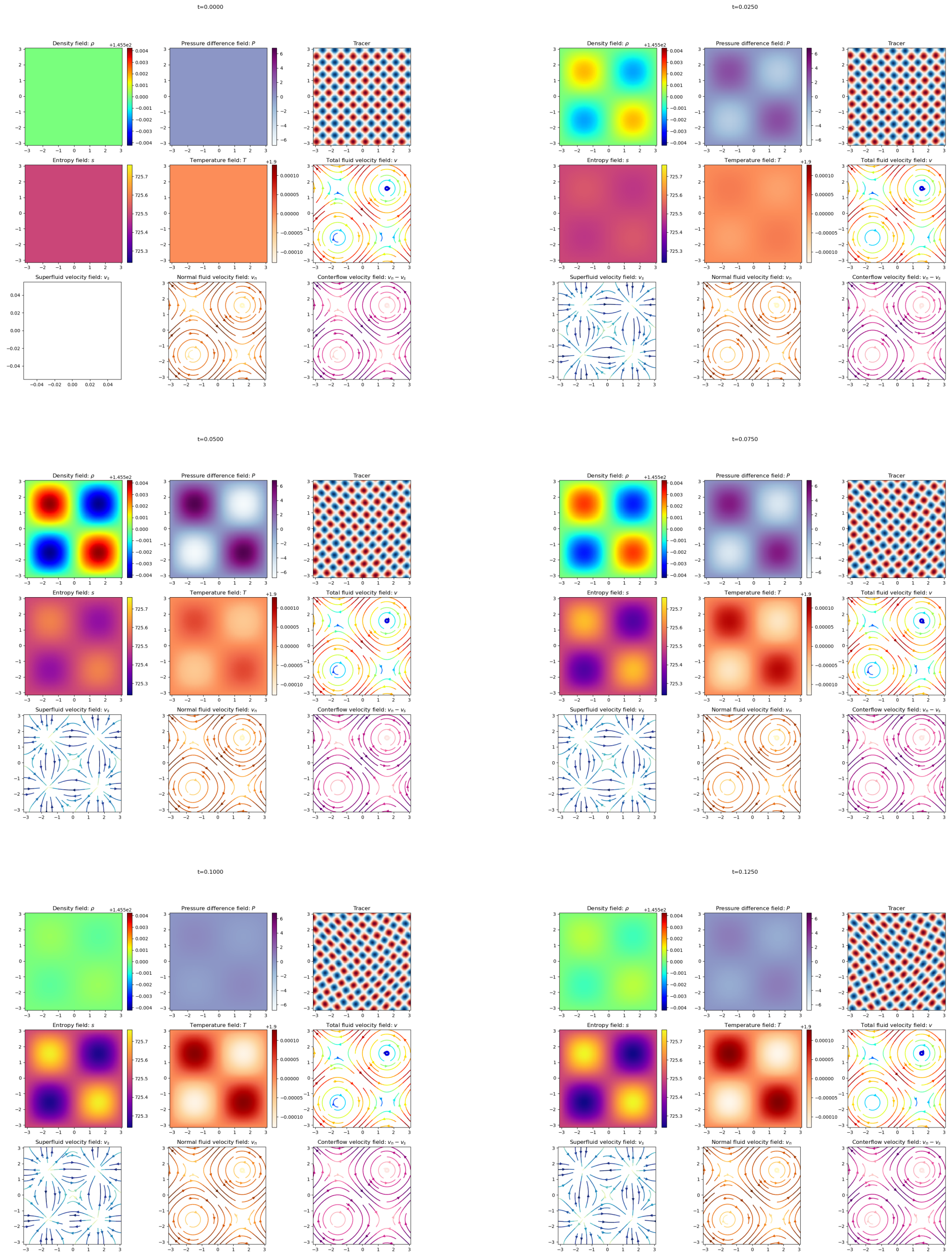

Figure 13: Snapshots from simulation 4

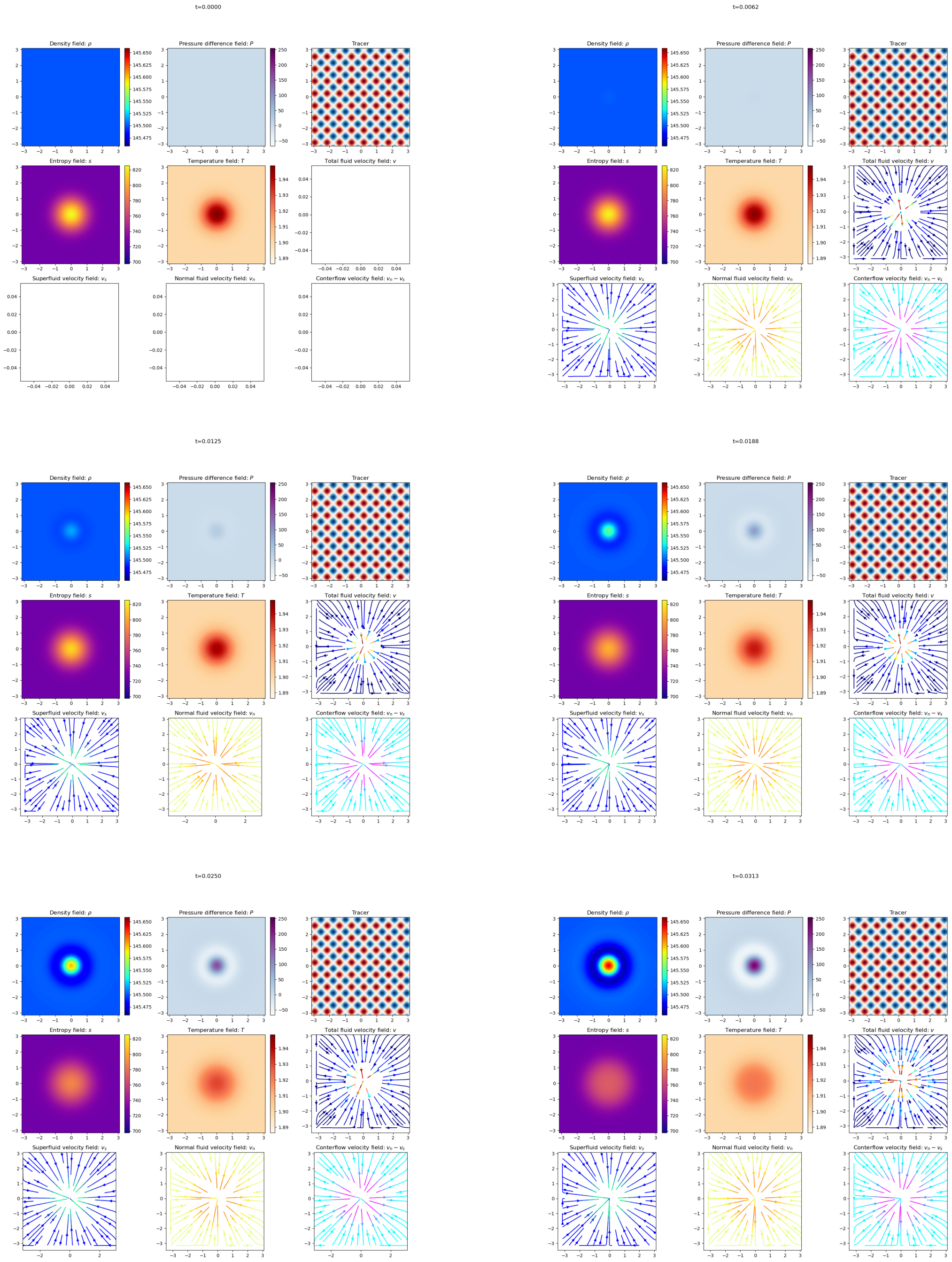

Figure 14: Snapshots from simulation 5